IEEE Access
Multidisciplinary | Rapid Review | Open Access Journal

Received October 22, 2019, accepted December 18, 2019, date of publication December 24, 2019, date of current version January 6, 2020.

Digital Object Identifier 10.1109/ACCESS.2019.2962058

A Novel Resilient Robot: Kinematic Analysis and Experimentation

FEI WANG[1], ZHIQIN QIAN[1], ZHIGUANG YAN[1], CHENWANG YUAN[3], AND WENJUN ZHANG[2,3], (Senior Member, IEEE)

[1]School of Mechanical and Power Engineering, East China University of Science and Technology, Shanghai 200237, China
[2]School of Mechatronic Engineering and Automation, Shanghai University, Shanghai 200444, China
[3]Department of Mechanical Engineering, University of Saskatchewan, Saskatoon, SK S7N5A9, Canada

Corresponding authors: Zhiqin Qian (qianzhiqin@ecust.edu.cn) and Wenjun Zhang (chrismzhang@hotmail.com)

This work was supported in part by the Shanghai Alliance Plan under Grant LM201622, and in part by the National Natural Science Foundation of China under Grant 51375166. The work of Wenjun Zhang was supported by the Discovery Grant from NSERC.

ABSTRACT A resilient robot is a robot that can recover its function after the robot is partially damaged. In this paper, a study of an under-actuated resilient robot with closed loops and passive joints is presented. First, a prototype system was built, which serves as a study vehicle and is called R-Robot II for short. Second, the kinematics of the prototype robot R-Robot II, necessarily for the change of the robot structure in, was developed. Finally, the experimentation of the R-Robot II was carried out. The result shows that the desired resilient behavior of R-Robot II can be exhibited. The architecture of R-Robot II, along with the design of the mechanical modules and simulation, was reported elsewhere. This paper focuses on the physical realization of R-Robot II and on the experimentation.

INDEX TERMS Resilient robot, D-H parameter method, topology, kinematic analysis.

I. INTRODUCTION

Resilience of machines was first elaborated in [21]. The name of resilient robot was perhaps first used in [4], though there is no definition on the concept of resilience in their paper [4]. Definition of the resilience to a much broader dynamic system, including manufacturing system, service system and supply system, has been widely discussed in the literature [13], [14], [19], [20], and it is defined as an ability of the system to recover its original function, which has been lost due to the external and internal disturbances, with its own resource and energy within a required period of time and an affordable cost. A resilient system is thus with a prolonged life expectancy and is extremely useful in a situation that a system is vulnerable and/or impossible to repair and/or unaffordable cost to repair. For example, the Mars launch reconnaissance vehicle of NASA was unable to move due to a wheel that fell into an unexpected soft soil, and eventually the mission was halted [8]. It is noted that in this paper, repair is considered as an activity that needs external resource and energy [19].

The associate editor coordinating the review of this manuscript and approving it for publication was Hamid Mohammad-Sedighi.

Two similar concepts with the concept of resilience are robustness and reliability. In brief, reliability is the life expectancy of a system determined at the design stage, and robustness is the ability of a system to resist disturbances that however do not cause the structural change of the system [19]. In literature, resilience is sometimes included in robustness or reliability [14], and robustness is included in resilience, particularly as the pre-stage of resilience [9].

Robots are a dynamic system and have several types of conceptual structures from certain perspectives. First, a robot has degrees of freedom (DOF), which is defined as the number of motors or actuators needed to make every link have a definite motion under the rigid body assumption [18]. Second, a robot has serial or open-loop structure, parallel structure, and closed-loop structure [1]. Third, a robot can include active joint (i.e., motor or actuator), passive joint (i.e., two links that are jointed can have a relative rotation or translation or cylindrical motion), and a fixed joint (i.e., two links that are joined into a definite angle and have no any relative motion). Fourth, a robot can have servomotor or varying speed motor or constant velocity motor [3], [12], [10]. Fifth, a robot can have different distributions of actuators or motors over joints (i.e., different inputs and different outputs) [18]. Sixth, a robot may include elements that the friction

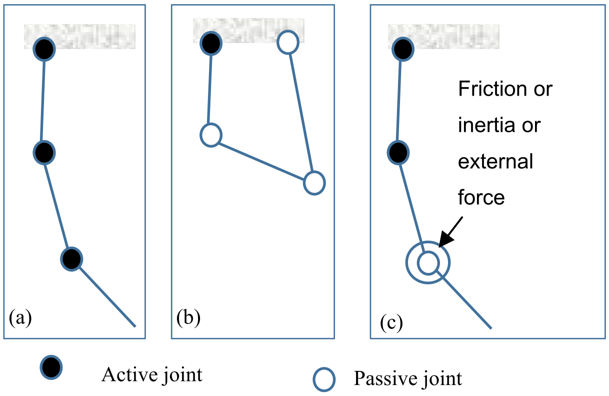

FIGURE 1. **The structure of under-actuated robot: (a) under-actuated robot; (b) close-looping in structure; (c) exerting force.**

plays an active in actuating motion, e.g., a wheeled robot with the wheel contacting with the ground to create a stick between the wheel and ground, which is called pure rotation, stick-slip actuated robot [22], [7].

Further, to a spatial robot, the end-effector has six degrees of freedom (DOF) (three rotations and three translations), and to a planar robot, the end-effector has three degrees of freedom (one rotation and two translations). To a serial structure, six motors are needed to make the end-effector to a motion of six degrees of freedom, while to a planar serial structure, three motors are needed to make the end-effector to a motion of three degrees of freedom. If the number of motors is less than six (three) in a serial spatial robot (in a serial planar robot), the robot is called under-actuated robot (Fig. 1a).

An under-actuated robot includes the link with no definite motion (Fig. 1a, Link 3) from a point of view of kinematics (i.e., DOF is less than 3 for a serial planar robot; DOF is less than 6 for a serial spatial robot). However, the motion of the link with un-definite motion may be determined through close-looping in structure (Fig. 1b) and forcing such as inertial force, friction force or additional force (Fig. 1c). A care needs to be taken that a robot may be a hybrid structure [1] and can still be under-actuated if a branch of the structure is a serial structure with its DOF less than 6 (spatial) or less than 3 (planar).

According to [17], the resilience of a robot can be attained by three approaches [16], [17]: (1) changing the principle that governs the motion behavior of a robot, e.g., from walking to crawling for advancement; (2) changing the topology or configuration of a robot; (3) changing the state of a robot. In [6], the three approaches are extended to five approaches; in addition to the foregoing three approaches, the other two approaches are: (4) changing the context of a robot, e.g., changing the way the robot interacts with the environment, and (5) changing the behavior of a robot, e.g., change the pair of states, from (state variable A, state variable B) to (state variable A, state variable C). In this paper, we consider the robot that may be under-actuated with a closed loop structure, fully-actuated with an open loop structure, or under-actuated with some components that have no definite motion.

In literature, self-reconfigurable robots are with the same capability of self-changing their configurations. For instance, CHOBIE designed by Michihiko KOSEKI belongs to a kind of lattice structure robot [5]. Each module in CHOBI has a sliding mechanism and can move forward with the translation of all modules. Although the lattice-structured robot is easy to realize self-reconfiguration, it has limitations in terms of the functionality of the robot. Conro designed by Andres Castano is a self-reconfigurable chain robot [2]. Conro modular robots can be reconfigured into different shapes, such as snake or quadruped, but their self-reconfiguration is a complex and slow process. SUPERBOT designed by Behnam Salemi of the University of Southern California uses a hybrid type structure [11]. A separate unit of SUPERBOT consists of two sub-modules and each with an anode joint and a cathode joint. This multi-sub-module bilateral system can enhance the self-reconfiguration performance of the robot system, but it has the disadvantage of poor mobility of independent units.

One of the important differences of self-reconfigurable robots in literature today other than the resilient robot developed in our work is that the former is composed of a set of active joints, while the latter (our robot) allows the passive joint and passive link, and subsequently closed loop with passive joint, in the robot. This feature improves the resilience of a robot in that if an active joint is broken to a passive joint, the whole robot may still work. It can be expected that the robot with this feature is with much lower cost than those self-reconfigurable robots which have all their joint modules active, meaning expensive servo-motors in there.

The remainder of this paper is structured as follows. Section II describes the architecture of a novel humanoid resilient robot. The kinematic analysis and simulation of the upper or lower arm of the robot are introduced in Section III. Section IV presents the physical realization of the module of the resilience robot and the test-bed. Section V presents the experimentation. Section VI is a conclusion.

II. ARCHITECTURE OF R-ROBOT II

R-robot II is a modular robot. It could have different configurations or shapes, e.g. humanoid robot, as shown in Fig. 2. For each module, it has one male surface (Fig. 3a) and three female surfaces (Fig. 3c). The detailed design of module can be found from our previous paper [15].

In the module of R-robot II there is an electronic clutch that can connect and disconnect the motor with drive shaft in the module to realize the change of the status of a module among the active joint, passive joint and fixed joint. This design provides more possibilities when the modules connect each other to form a richer structure of a robot, compared with the existing self-reconfigurable robot in literature. It is noted that when forming a robot, the male surface of a module connects with a female surface of another module.

Back to Fig. 2, it shows how a humanoid robot recovers from a damage. Fig. 2a shows the right half of a humanoid robot. The right arm of the robot should have four modules as the right leg. Yet, suppose the last module (M7') of the

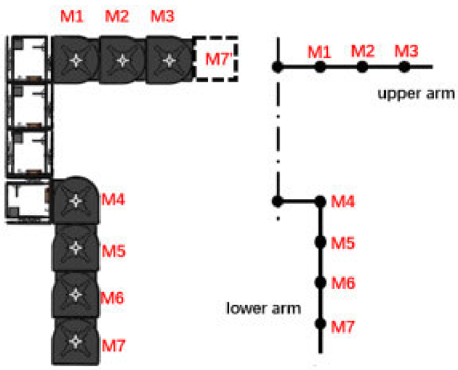

(a) (b)

FIGURE 2. The simplified R-Robot II arms: (a) 3D model; (b) simplified model.

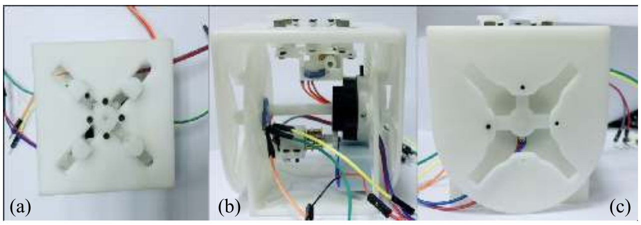

FIGURE 3. Completed module: (a) top view; (b) front view; (c) side view.

right arm is lost. In this case, to keep the function of the robot, the robot needs to move the last module (M7) on the right leg to the right arm replacing the lost module M7'.

To move the module M7 to M7', there are mainly three steps: (1) to connect the right arm with the right leg; (2) to connect module M7 with module M3; (3) to disconnect the right arm with the right leg at the module 6. After that, the change process or recovery process is completed. It is noted that in the first two steps, there are actually an infinite number of possibilities due to an infinite number of possibilities for the module M3 and module 7 to meet and to be assembled. However, to determine which possibility is the best is out of the scope of this paper. In the present paper, the situation is considered where a particular assembly positon and orientation for the module 3 and module 7 are given.

To a particular docking or assembly position and orientation for the module 3 and module 7, the kinematic analysis of the arm (M1-M3, 3R robot for short) and leg (M4-M7, 4R robot for short) is needed to find the joint angles of the sub-robots, respectively. With the joint angle information, the sub-robots can then bring the module 3 and module 7 to the assembly position and orientation to assemble them.

III. KINEMATIC ANALYSIS

In this section, a separate discussion on the upper arm or sub-robot 3R and lower arm or sub-robot 4R is presented.

A. FORWARD KINEMATICS OF THE UPPER ARM

The D-H coordinate system is established on the upper arm (Fig. 4). The axes of all the joints of the upper arm are perpendicular to the paper plane because the robot is a planner robot. According to the D-H coordinate system as established, all the link offset distances di (i=1, 2, 3) are 0, and so are the angle between any adjacent Z-axis, i.e., αi (i=1, 2, 3) is 0. The distance between any adjacent Z-axes is L1, L2, and L3, respectively and they are constants. The variables are the angles between any adjacent X-axes, i.e., θ, θ, θ, respectively. The upper arm extremity, i.e., the coordinate system {3} relative to the reference coordinate system {0}, can be expressed by

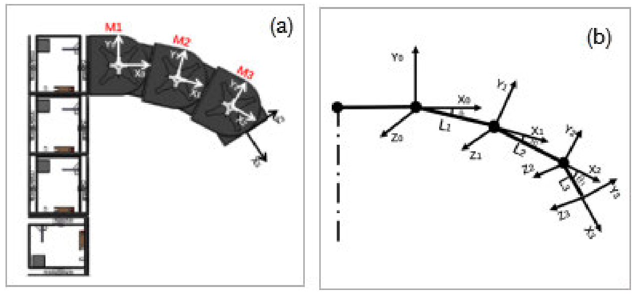

FIGURE 4. R-Robot II upper arm space coordinate system: (a) establish upper arm coordinate system; (b) simplified coordinate system.

$$ {}^{0}_{3}T = \begin{bmatrix} T_{11} & T_{12} & 0 & T_{14} \\ T_{21} & T_{22} & 0 & T_{24} \\ 0 & 0 & 1 & 0 \\ 0 & 0 & 0 & 1 \end{bmatrix} \tag{1} $$

The following equations based on the elements of Equation (1) can be found, i.e.:

$$ \begin{cases} T_{11} = -c\theta_3(s\theta_1 s\theta_2 - c\theta_1 c\theta_2) - s\theta_3(c\theta_1 s\theta_2 + c\theta_2 s\theta_1) \\ T_{12} = s\theta_3(s\theta_1 s\theta_2 - c\theta_1 c\theta_2) - c\theta_3(c\theta_1 s\theta_2 + c\theta_2 s\theta_1) \\ T_{14} = L_1 + L_2 c\theta_1 - L_3(s\theta_1 s\theta_2 - c\theta_1 c\theta_2) \\ T_{21} = c\theta_3(c\theta_1 s\theta_2 + c\theta_2 s\theta_1) - s\theta_3(s\theta_1 s\theta_2 - c\theta_1 c\theta_2) \\ T_{22} = -c\theta_3(s\theta_1 s\theta_2 - c\theta_1 c\theta_2) - s\theta_3(c\theta_1 s\theta_2 + c\theta_2 s\theta_1) \\ T_{24} = L_2 s\theta_1 + L_3(c\theta_1 s\theta_2 - c\theta_2 s\theta_1) \end{cases} \tag{2} $$

where c represents the cosine function, and s represents the sine function.

The Robotic Toolbox in MATLAB was actually employed to solve the above equations. The 'Seriallink.plot' function of the Robotic Toolbox is used to visualize the result of the forward kinematic analysis (Fig. 5).

B. INVERSE KINEMATICS OF THE UPPER ARM

In the change process for a resilient robot, the problem is: given the position and orientation of a module, find the joint angles of the sub-robot that drives this module. This problem refers to inverse kinematics of a robot.

Taking a particular situation as an example. In this situation, the angle of the mating surface of M3 with respect to the y0 of the global coordinate system is taken as 60° (see Fig. 6). The origin of the local coordinate system {3} with respect to the global coordinate system {0} are 169.88mm and 87.24mm. The foregoing information can be written as a

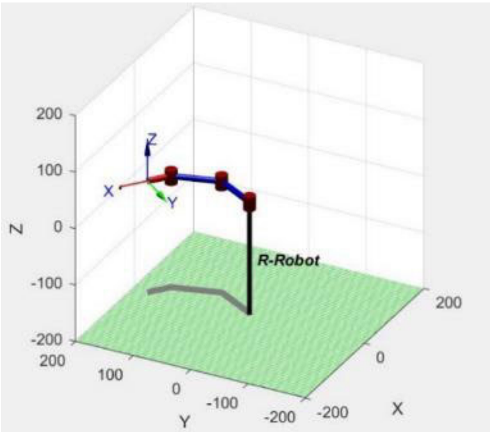

FIGURE 5. Pose solution of R-Robot II upper arm by positive kinematics.

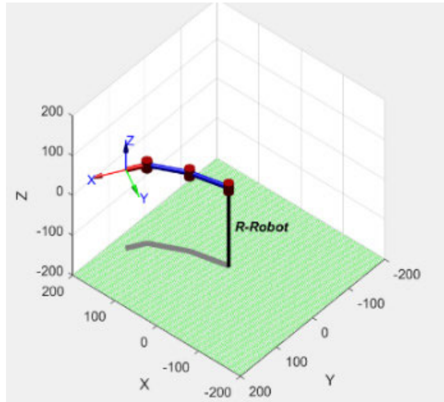

FIGURE 7. R-Robot II arm pose based on inverse kinematics.

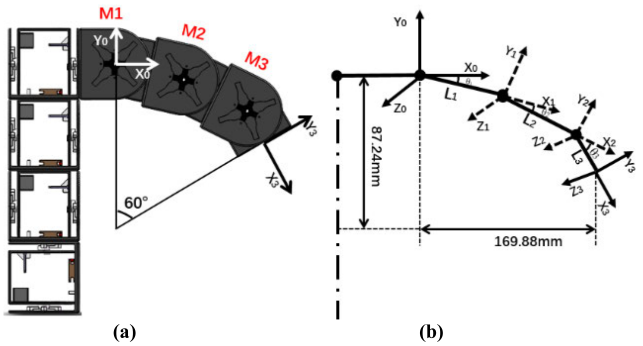

FIGURE 6. The pose of R-Robot II upper arm end actuator and its coordinate system: (a) End effector pose (b) coordinate system.

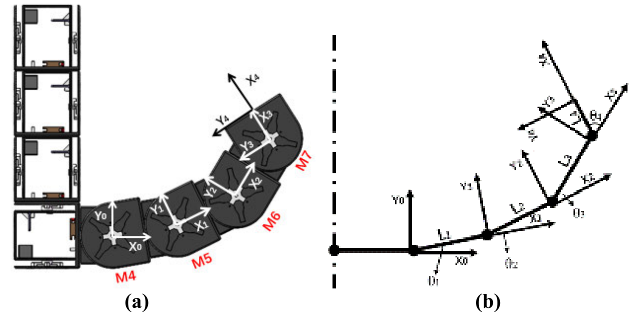

FIGURE 8. The coordinate system establishment of R-Robot II lower arm joints: (a) coordinate system of lower arm; (b) simplified coordinate system.

matrix, i.e.:

$$ {}^0_3T = \begin{bmatrix} \cos 60^0 & -\sin 60^0 & 0 & 169.88mm \\ \sin 60^0 & \cos 60^0 & 0 & 87.24mm \\ 0 & 0 & 1 & 0 \\ 0 & 0 & 0 & 1 \end{bmatrix} \tag{3} $$

The joint angles of the links ($\theta_1, \theta_2, \theta_3$) can be found from Equation (2), i.e.:

$$ \begin{cases} -c\theta_3(s\theta_1 s\theta_2 - c\theta_1 c\theta_2) - s\theta_3(c\theta_1 s\theta_2 + c\theta_2 s\theta_1) = \cos 60^0 \\ s\theta_3(s\theta_1 s\theta_2 - c\theta_1 c\theta_2) - c\theta_3(c\theta_1 s\theta_2 + c\theta_2 s\theta_1) = -\sin 60^0 \\ L_1 + L_2 c\theta_1 - L_3(s\theta_1 s\theta_2 - c\theta_1 c\theta_2) = 169.88mm \\ c\theta_3(c\theta_1 s\theta_2 + c\theta_2 s\theta_1) - s\theta_3(s\theta_1 s\theta_2 - c\theta_1 c\theta_2) = \sin 60^0 \\ -c\theta_3(s\theta_1 s\theta_2 - c\theta_1 c\theta_2) - s\theta_3(c\theta_1 s\theta_2 + c\theta_2 s\theta_1) = \cos 60^0 \\ L_2 s\theta_1 + L_3(c\theta_1 s\theta_2 - c\theta_2 s\theta_1) = 87.24mm \end{cases} \tag{4} $$

The above equation was solved in MATLAB. The result can be plotted with the function 'robot.plot'; see Fig. 7.

C. FORWARD KINEMATICS OF THE LOWER ARM

The lower arm of the sub-robot is a 4R (Fig. 8a). The D-H coordinate system is established on the lower arm, and the result is shown in Fig. 8b. The kinematic equation is shown below:

$$ {}^0_4T = \begin{bmatrix} T_{11} & T_{12} & 0 & T_{14} \\ T_{21} & T_{22} & 0 & T_{24} \\ 0 & 0 & 1 & 0 \\ 0 & 0 & 0 & 1 \end{bmatrix} \tag{5} $$

In Equation (5), the joint angles are known, and by using the Robotic toolbox of MATLAB, the pose of the end-effector can be found. Fig. 9a plots the lower arm, and Fig. 9b shows adjusting the joint angle with the function 'SerialLink.teach'.

D. INVERSE KINEMATICS OF THE LOWER ARM

Corresponding to the particular situation as discussed for the upper arm, the pose of the docking plane of the module M7 is as follows (Fig. 10): the orientation of M7 is 120°, and the coordinates of the origin of the local coordinate system {4} with respect to the global coordinate system {0} are 169.88 mm and 152.21mm. This information can be represented by

$$ {}^0_4T = \begin{bmatrix} \cos 120^0 & -\sin 120^0 & 0 & 169.88mm \\ \sin 120^0 & \cos 120^0 & 0 & 152.21mm \\ 0 & 0 & 1 & 0 \\ 0 & 0 & 0 & 1 \end{bmatrix} \tag{6} $$

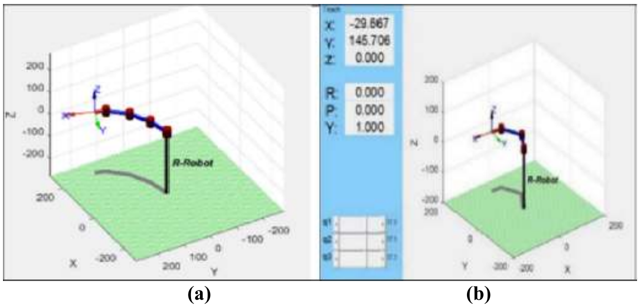

FIGURE 9. The operating arm model in MATLAB: (a) The pose solution of R-Robot II lower arm by positive kinematics; (b) Manipulator teaching system.

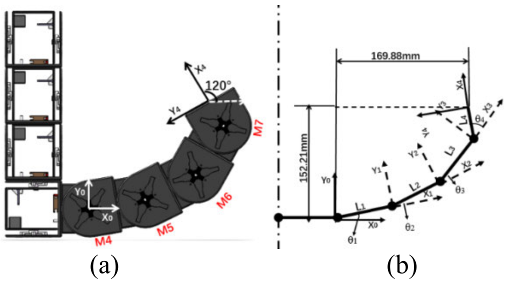

FIGURE 10. The coordinate system establishment of R-Robot II lower arm joints: (a) the pose of end actuator; (b) The establishment of a coordinate system.

$$\begin{cases} T_{11} = \cos 120^0 \\ T_{12} = -\sin 120^0 \\ T_{14} = 169.88mm \\ T_{21} = \sin 120^0 \\ T_{22} = \cos 120^0 \\ T_{24} = 152.21mm \end{cases} \tag{7}$$

The 'ikine' function in the Robotic Toolbox was employed to solve the above inverse kinematics problem, resulting in the joint angles as T2 = [0.163, 0.291, 0.607, 1.034]. It is noted that this is one of the inverse kinematic solutions. Fig. 11 shows the plot of the result.

IV. PHYSICAL REALIZATION

The detailed design of the module can be found from our previous paper [Yuan]. Fig. 12 shows the module components fabricated by 3D printing. They can be assembled into function modules (Fig. 3).

The logical diagram of all the components in the test-bed system is shown in Fig. 13. In this figure, the component 'regulator module' is to stabilize the voltage out of the component 'power supply'. The 'power supply' drives the component of 'relay' in the microprocessor (MCU). The microprocessor has three parts to control the motor, wireless communication module, and electromagnetic clutch in the robot module, respectively. The MCU on one hand instructs the motor while on the other hand the potentiometer of the motor sends the signal back to the MCU, which is the angular displacement of the motor.

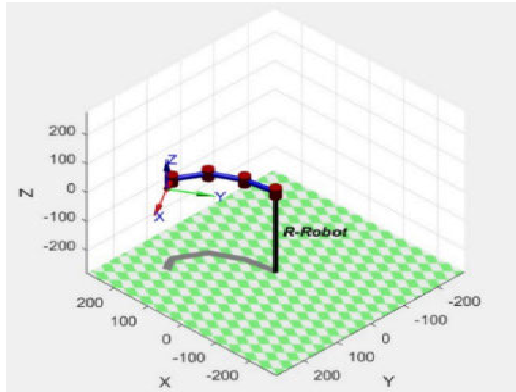

FIGURE 11. Lower arm pose based on inverse kinematics of R-Robot II.

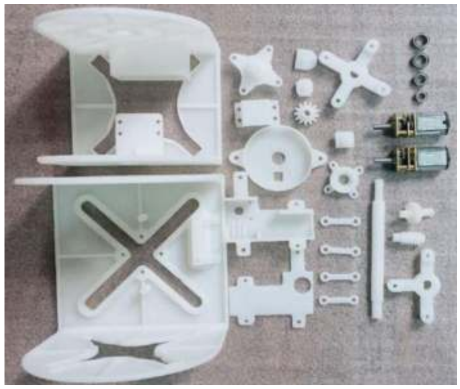

FIGURE 12. Components and parts for R-Robot II.

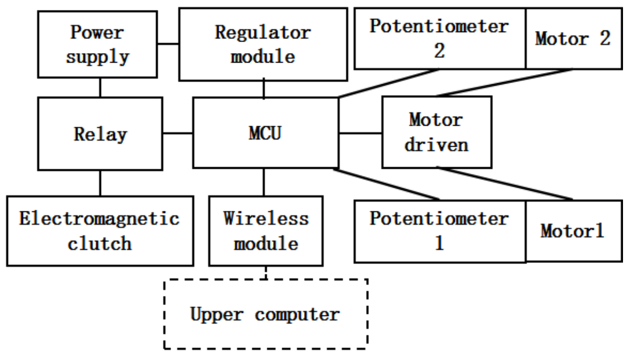

FIGURE 13. The hardware layout of module unit.

It is noted that the communication between the robotic module and upper computer is via wireless. Bluetooth was used to transmit the information between the slave computer and the host computer. The test-bed system used in the upper computer was Arduino IDE. The angular displacement of the motor was sensed in real time via the serial monitor in the Arduino IDE (Nano3.0). As such, the negative feedback control of the DC motor was realized in the test-bed system. The electric circuit system is shown in Fig. 14.

V. EXPERIMENTATION

The physical test-bed system is shown in Fig. 15, where there is a host computer, the Arduino micro-controller, and modules of R-Robot II.

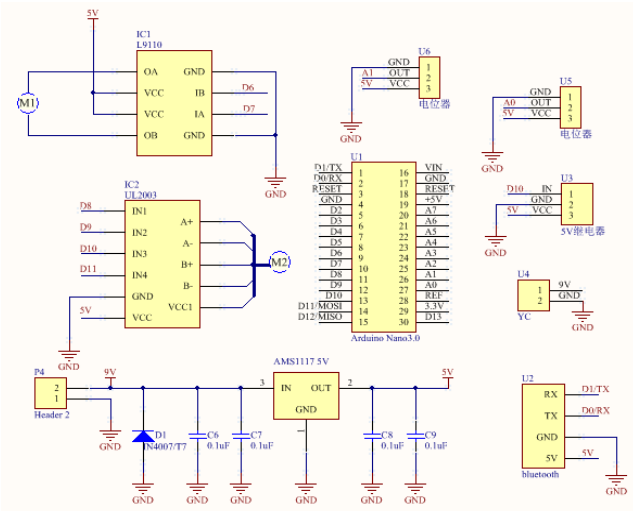

FIGURE 14. The overall hardware circuit design.

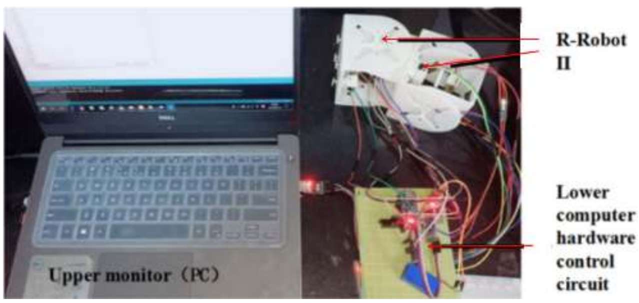

FIGURE 15. Overall experimental test platform.

TABLE 1. Calibration data of joint-angel sensor.

Angel (°)	First group U(mV)	Second group U(mV)	Third group U(mV)	Fourth group U(mV)	Fifth group U(mV)
0	256	253	255	258	260
20	310	311	310	312	307
40	368	364	370	365	367
60	424	423	421	424	424
80	477	475	479	476	481
90	511	508	512	514	510
100	535	530	534	540	537
120	596	602	604	594	593
140	650	647	652	651	645
160	699	702	695	697	698
170	725	721	720	727	729

A. SINGEL MODULE EXPERIMENT

The purpose of a single module testing is to confirm the proper functioning with the sensor and driver. To calibrate the sensor in the motor, the angular displacement ranges from 0 to 170° without loss of generality, and five sets of data were collected. Table 1 shows the relationship between the measured voltage value from the sensor and the reading of the joint angle. A linear regression was then performed to get

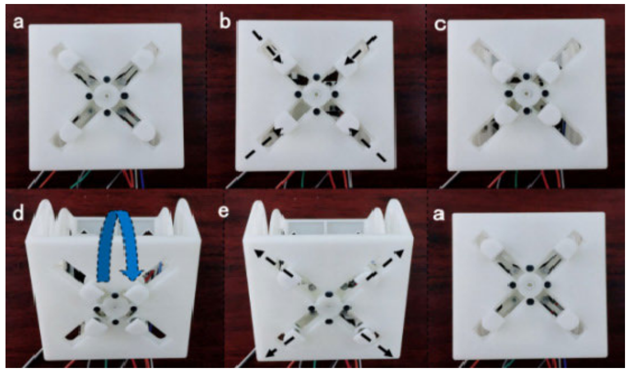

FIGURE 16. Single module work process demo: (a) initial posture; (b-c) male joint shrinkage; (d) module joint angle rotate 30°; (e) male connector opened.

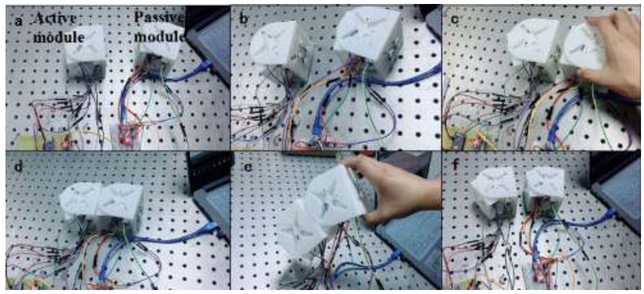

FIGURE 17. The two modules are connected to separate: (a) Initial state; (b) Active module rotate a joint angle, Active module anode joint shrinkage; (c) Man-assisted module movement; (d) Two-module connection; (e) connection success; (f) Separation of two modules.

TABLE 2. Calibration data of connector sensor.

Motion	First group U(mV)	Second group U(mV)	Third group U(mV)	Fourth group U(mV)	Fifth group U(mV)	Average value U(mV)
shrink	23	22	23	24	21	23
expansion	936	936	935	936	937	936

the calibration equation, i.e.:

$$y = 2.781x + 256.75 \tag{8}$$

where x stands for voltage value measured by sensor, and y stands for the joint angle.

The connector has two states: expansion and shrinkage. The relationship of the two states with the data measured from the sensor is shown in Table 2.

The result of the testing of the module is shown in Fig. 16. Specifically, Fig. 16a shows the initial state of the module, at which, the joint angle of the module is 0 and the anode grapple is in the open state. At this time, the motor in the module actuates the anode grapple to the state of Fig. 16b, and then to the state of Fig. 16c, which is the extreme closed position. After that, rotate the joint module by 30° to the state of Fig. 16d. At this time, the anode grapple is opened to its extreme open state of Fig. 16e. Finally, rotate the module in the opposite direction by 30° and the module goes back to the initial state of Fig. 16a. Then the module's working condition test was completed.

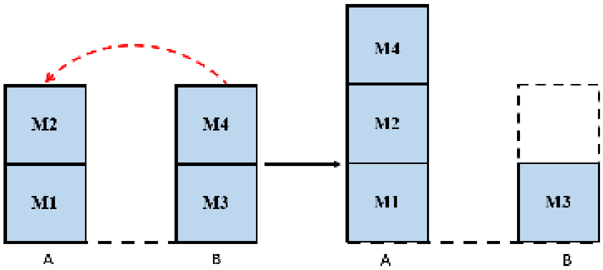

FIGURE 18. Experimental design of multi-module.

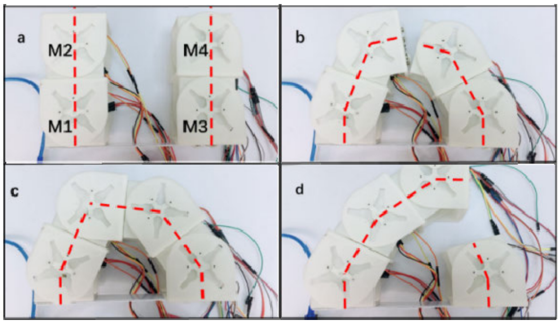

FIGURE 19. Experimental design of multi-module: (a) Initial state; (b-c) Module joint angle rotates and docking process completed; (d) Modules M3 and M4 are separated and module M4 is migrated to left.

B. TWO-MODULE EXPERIMENT

This experiment is expected to test the docking and undocking process. Two modules were used in the experiment, one of which is an active module (left in Fig. 17) and the other is a passive module (right in Fig. 17). Fig. 17a shows the initial situation of the two modules. In Fig. 17b, the joint in the active module is rotated by 30° and the module is contracted. Manually move the passive joint module close to the active joint module (Fig. 17c). Fig. 17d shows that the active joint module successfully docks with the passive joint module. Fig. 17e shows the active joint module rotates the passive joint module to a certain orientation to demonstrate the strength of the connection. Fig. 17f shows the two modules are undocked to their initial situation.

C. MULTI-MODULE EXPERIMENT

The purpose of this testing is to demonstrate the change of the structure of the robot which has two groups of modules (Fig. 18, Group A and Group B). The process is to make the following operations: to dock M2 in Group A to M4 in Group B, to undock M4 from M3, and finally to bring M4 to Group A. Fig. 19 shows the process on the physical modules.

VI. CONCLUSION

This paper presented an on-going study of resilient robots with the passive joint and passive link and under-actuated structure. In our precious work, the architecture of this resilient robot was discussed along with the design of the basic module of the robot. This paper presented the physical realization of the module, kinematics necessary for changing the structure, and experimentation. Specifically, the experimentation was performed on a single module for its function along with the sensor for measuring the position, two modules for their connection and disconnection functions, and four modules to demonstrate moving one module from one group to another group by a sub-robot of the robot.

A conclusion can be drawn that the proposed concept of the resilient robot is feasible. The resilient robot is different from the self-reconfigurable robot in that the former is more general in terms of the structure change while the latter changes the system connectivity only. In terms of the structure of a robot, the resilient robot includes the passive joint and passive link, which allows the possibility that the system may still work even the actuator is damaged, especially degrading to a resolute joint (passive joint); while the self-reconfigurable robot is composed of modules that have the actuator and controller, or self-controlled and autonomous modules.

REFERENCES

[1] Z. Bi, Y. Lin, and W. Zhang, "The general architecture of adaptive robotic systems for manufacturing applications," *Robot. Comput.-Integr. Manuf.*, vol. 26, no. 5, pp. 461–470, Oct. 2010.

[2] A. Castano, R. Chokkalingam, and P. Will, "Autonomous and self-sufficient conro modules for reconfigurable robots," in *Proc. Distrib. Auton. Robot. Syst. 4*, Sep. 2000, pp. 155–164.

[3] L. Cheng, Y. Lin, Z.-G. Hou, M. Tan, J. Huang, and W. J. Zhang, "Adaptive tracking control of hybrid machines: A closed–chain five–bar mechanism case," *IEEE/ASME Trans. Mechatronics*, vol. 16, no. 6, pp. 1155–1163, Dec. 2011.

[4] R. Cohen, M. G. Lipton, M. Q. Dai, and B. Benhabib, "Conceptual design of a modular robot," *J. Mech. Des.*, vol. 114, no. 1, pp. 117–125, Mar. 1992.

[5] M. Koseki, K. Minami, and N. Inou, "Cellular robots forming a mechanical structure," in *Proc. Distrib. Auton. Robot. Syst. 6*, Sep. 2007, pp. 139–148.

[6] J. K. Liu, C. L. Liu, C. W. Yuan, Z. Q. Qian, W. J. Zhang, and B. Zhang, "ReBot: A novel under-actuated resilient robot," in *Proc. IEEE 25th Int. Conf. Mechatronics Mach. Vis. Pract. (M2VIP)*, Stuttgart, Germany, Nov. 2018, pp. 1–6.

[7] Y. F. Liu, J. Li, X. H. Hu, Z. M. Zhang, L. Cheng, Y. Lin, and W. J. Zhang, "Modeling and control of piezoelectric inertia-friction actuators: Review and future research directions," *Mech. Sci.*, vol. 6, no. 2, pp. 95–107, Jul. 2015.

[8] *Mars Exploration Rovers Overview*. Accessed: Jan. 12, 2018. [Online]. Available: https://mars.nasa.gov/mer/mission/overview/

[9] C. Nan and G. Sansavini, "A quantitative method for assessing resilience of interdependent infrastructures," *Rel. Eng. Syst. Saf.*, vol. 157, pp. 35–53, Jan. 2017.

[10] P. Ouyang, Q. Li, W. Zhang, and L. Guo, "Design, modeling and control of a hybrid machine system," *Mechatronics*, vol. 14, no. 10, pp. 1197–1217, Dec. 2004.

[11] B. Salemi, M. Moll, and W.-M. Shen, "SUPERBOT: A deployable, multi–functional, and modular self–reconfigurable robotic system," in *Proc. IEEE/RSJ Int. Conf. Intell. Robots Syst.*, Oct. 2006, pp. 3636–3641.

[12] Z. Sun, B. Zhang, L. Cheng, and W. Zhang, "Application of the redundant servomotor approach to design of path generator with dynamic performance improvement," *Mech. Mach. Theory*, vol. 46, no. 11, pp. 1784–1795, Nov. 2011.

[13] J. Wang, R. Dou, R. Muddada, and W. Zhang, "Management of a holistic supply chain network for proactive resilience: Theory and case study," *Comput. Ind. Eng.*, vol. 125, pp. 668–677, Nov. 2018.

[14] J. Wang, R. R. Muddada, H. Wang, J. Ding, Y. Lin, C. Liu, and W. Zhang, "Toward a resilient holistic supply chain network system: Concept, review and future direction," *IEEE Syst. J.*, vol. 10, no. 2, pp. 410–421, Jun. 2016.

[15] C. W. Yuan, R. X. Yin, W. J. Zhang, and G. Chen, "A new under-actuated resilient robot," in *Proc. IEEE Int. Conf. Syst., Man, Cybern. (SMC)*, Banff, AB, Canada, Oct. 2017, pp. 1202–1207.

[16] T. Zhang, W. Zhang, and M. Gupta, "Resilient robots: Concept, review, and future directions," *Robotics*, vol. 6, no. 4, p. 22, Sep. 2017.

[17] T. Zhang, W. Zhang, and M. M. Gupta, "An underactuated self-reconfigurable robot and the reconfiguration evolution," *Mech. Mach. Theory*, vol. 124, pp. 248–258, Jun. 2018.
[18] W. J. Zhang and Q. Li, "On a new approach to mechanism topology identification," *ASME Trans., J. Mech. Des.*, vol. 121, no. 1, pp. 57–64, Mar. 1999.
[19] W. J. Zhang and Y. Lin, "On the principle of design of resilient systems—Application to enterprise information systems," *Enterprise Inf. Syst.*, vol. 4, no. 2, pp. 99–110, May 2010.
[20] W. J. Zhang and C. A. van Luttervelt, "Toward a resilient manufacturing system," *CIRP Ann.*, vol. 60, no. 1, pp. 469–472, 2011.
[21] Z.-H. Sun, G. S. Yang, B. Zhang, and W.-J. Zhang, "On the concept of the resilient machine," in *Proc. 6th IEEE Conf. Ind. Electron. Appl. (ICIEA)*, Beijing, China, Jun. 2011, pp. 357–360.
[22] Z. M. Zhang, Q. An, J. W. Li, and W. J. Zhang, "Piezoelectric friction–inertia actuator—A critical review and future perspective," *Int. J. Adv. Manuf. Technol.*, vol. 62, nos. 5–8, pp. 669–685, Sep. 2012.

FEI WANG received the bachelor's degree from the East China University of Technology, in 2017, where he is currently pursuing the master's degree with the College of Mechanical and Power Engineering. He is currently a Research Assistant with The Complex and Intelligent Systems Research Group. His research interests include mechatronics, system control, and robot structure design. He has received the Academic Scholarship and the Inspirational Scholarship from the University.

ZHIQIN QIAN received the B.Eng. and M.S. degrees in mechanical engineering from Zhengzhou University, China, in 1993 and 1998, respectively, and the Ph.D. degree in mechanical engineering from the Dalian University of Technology, China, in 2001. She is currently an Associate Professor with the School of Mechanical and Power Engineering, East China University of Science and Technology, China. She has authored or coauthored more than 60 technical articles in journals and conference proceedings in the area of mechatronics, including medical robotics and human–robot interactive systems. Her research interests include optimization, fault diagnosis, modeling, and control of mechatronic systems with emphasis on medical robotics.

ZHIGUANG YAN received the bachelor's degree in mechanical design and manufacturing and automation and the master's degree in mechanical engineering from the East China University of Science and Technology, in 2015 and 2018, respectively. He was working on the research of complex and intelligent systems, from 2015 to 2018. He is currently works at the School of Mechanical and Power Engineering, East China University of Science and Technology. His research interests include robot structure design and algorithm of intelligent control. He has received multiple scholarships and outstanding students' awards from University.

CHENWANG YUAN received the bachelor's and M.Sc. degrees in mechanical engineering from Donghua University, China, in 2014 and 2017, respectively. He is currently pursuing the Ph.D. degree with the Department of Mechanical Engineering, University of Saskatchewan, Canada. His research interests include soft robotics, mechanical design, soft sensor, and mechatronic system control.

WENJUN ZHANG (Senior Member, IEEE) received the Ph.D. degree from the Delft University of Technology, Delft, The Netherlands, in 1994. He is currently a Full Professor with the Department of Mechanical Engineering and the Division of Biomedical Engineering, University of Saskatchewan, Saskatoon, SK, Canada. He is also currently a Full Professor with the School of Mechatronic Engineering and Automation, Shanghai University. He has published more than 270 technical articles in peer-refereed journals or magazines and more than 150 technical articles in peer-refereed conference proceedings. His current research interests include informatics, design, modeling, and control of micro-motion systems, and modeling and management of large complex systems, such as socio-tech and physical–biological systems and human systems. He is also a Fellow of the Canadian Academy of Engineering owing to his outstanding work on resilience engineering and ASME. He is currently a Senior Editor of the IEEE/ASME TRANSACTIONS ON MECHATRONICS.